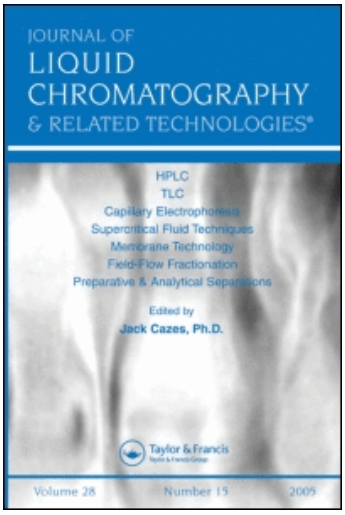

Journal of Liquid Chromatography & Related Technologies
Publication details, including instructions for authors and subscription information:
http://www.informaworld.com/smpp/title~content=t713597273

Separation and Quantitation of Silver Nanoparticles using Sedimentation Field-Flow Fractionation

Sun Tae Kim[a]; Dong Young Kang[a]; Seungho Lee[a]; Won-Suk Kim[b]; Jong Taik Lee[b]; Hye Sung Cho[b]; Sang Ho Kim[b]
[a] Department of Chemistry, Hannam University, Daejeon, Republic of Korea [b] Corporate R&D, LG Chem., Ltd., Daejeon, Republic of Korea

To cite this Article Kim, Sun Tae , Kang, Dong Young , Lee, Seungho , Kim, Won-Suk , Lee, Jong Taik , Cho, Hye Sung and Kim, Sang Ho(2007) 'Separation and Quantitation of Silver Nanoparticles using Sedimentation Field-Flow Fractionation', Journal of Liquid Chromatography & Related Technologies, 30: 17, 2533 — 2544
To link to this Article: DOI: 10.1080/10826070701540092
URL: http://dx.doi.org/10.1080/10826070701540092

Journal of Liquid Chromatography & Related Technologies®, 30: 2533–2544, 2007

ISSN 1082-6076 print/1520-572X online
DOI: 10.1080/10826070701540092

Separation and Quantitation of Silver Nanoparticles using Sedimentation Field-Flow Fractionation

Sun Tae Kim, Dong Young Kang, and Seungho Lee
Department of Chemistry, Hannam University, Daejeon, Republic of Korea

Won-Suk Kim, Jong Taik Lee, Hye Sung Cho, and Sang Ho Kim
Corporate R&D, LG Chem., Ltd., Daejeon, Republic of Korea

Abstract: Sedimentation field-flow fractionation (SdFFF) provides a mass based separation, and, thus, a size based separation for particles of uniform density. In this study, SdFFF was employed for separation and determination of size distributions of silver nanoparticles of about 100 nm in diameter. The relative abundances of each population in binary mixtures of silver nanoparticles were determined by mathematically deconvoluting the SdFFF fractograms. Various experimental parameters, including the field strength (channel rotation rate), flow rate, and the carrier composition, were varied to find an optimum SdFFF condition for separation and analysis of silver nanoparticles. The field and/or flow programming were also tested to improve the resolution. The silver nanoparticles were not resolved well when pure water was used as the carrier, due to charge interactions among the particles and between the particles and the channel wall. Water with 0.1% FL-70 was chosen as the dispersing medium and also as the carrier for SdFFF analysis of silver nanoparticles.

Keywords: Sedimentation field-flow fractionation (SdFFF), Silver nanoparticle, Particle-particle interaction, Deconvolution, Flow, and/or Field programming

Address correspondence to Seungho Lee, Department of Chemistry, Hannam University, 461-6 Junmin-dong, Daejeon 305-811, Republic of Korea. E-mail: slee@hannam.ac.kr

INTRODUCTION

Metal nanoparticles have wide ranging implications in various areas, including physics, chemistry, electronics, optics, material, and biomedical sciences. Various properties of metal nanoparticles depend on their morphology (e.g., size and shape), and significant effort has been made to develop a method to control the morphology of the particle.[1–4] Silver nanoparticles have extensive use in many applications. They can be used for antibacterial, antistatic, superconducting, biosensor, and catalytic materials.[5–8]

Field-Flow Fractionation (FFF) is a family of separation techniques that employs a combination of an external field and a liquid flow,[9] and is useful for separation and characterization of colloidal particles,[10,11] polymers,[12,13] and biological macromolecules.[14,15]

Sedimentation FFF (SdFFF) is particularly useful for separation of nano-sized colloidal particles. SdFFF has been used for separation and sizing of a variety of particulate samples including metal particles,[16] diesel soot,[17] titanium oxide particles of submicron sizes,[18] and zirconia.[19] The potential of SdFFF for analysis of silver nanoparticles has been previously shown.[20,21]

In this study, silver nanoparticles were synthesized and then analyzed by SdFFF. The aim of this study is to develop an SdFFF method for separation and determination of the mean size and the size distributions of silver nanoparticles.

THEORY

In FFF, the degree of retention is measured by the retention ratio R from the void time of the channel, t^0 and the retention time of the sample, t_r by:[10,22,23]

$$R = \frac{t^0}{t_r} \tag{1}$$

Theoretically, R is expressed as a function of a retention parameter λ by:

$$R = 6\lambda\left[\coth\left(\frac{1}{2\lambda}\right) - 2\lambda\right] \tag{2}$$

The dimensionless parameter, λ is given in SdFFF by:

$$\lambda = \frac{kT}{Fw} = \frac{kT}{m|1 - (\rho/\rho_\rho)|Gw} \tag{3}$$

where k is the Boltzmann constant, T the temperature, F the centrifugal force on the sample, w the channel thickness, m the particle mass, ρ and ρ_ρ the

density of the solvent and the sample, G the centrifugal acceleration, respectively. For spherical particles having the diameter d, Eq. (3) becomes:

$$\lambda = \frac{6kT}{\pi d^3 |\rho_\rho - \rho| Gw} \tag{4}$$

Thus, by measuring the retention time t_r, retention ratio R is determined by Eq. (1), then λ by Eq. (2), and finally the diameter d of the sample by:

$$d = \left(\frac{6kT}{\pi Gw \lambda \Delta\rho} \right)^{1/3} \tag{5}$$

EXPERIMENTAL

Materials

Polystyrene latex standards having the nominal diameters of 222, 300, and 502 nm were obtained from Duke Scientific (Palo Alto, CA). The density of polystyrene latex standard is known to be 1.05 g/mL. Four batches (batch I∼IV) of silver nanoparticles having different sizes were synthesized, from which six samples (Sample A∼F) were prepared. Sample A and E were prepared by dispersing 0.3 g of the batch I and batch II in 2 mL ethanol, respectively. Samples B, C, and D were prepared by mixing the sample A and E at the volume ratio of 80/20, 50/50, and 20/80, respectively. Sample F was prepared by mixing the suspensions of the batch III (0.5 g/2 mL) and IV (0.5 g/2 mL) at the volume ratio of 20/80. As shown in Figure 1, both batch I and II of the silver nanoparticles have broad size distributions ranging about 20∼100 and 60∼150 nm, respectively. The mean diameters measured by field emission scanning electron microscopy (FE-SEM) were about 70 and 145 nm, respectively, for batch I and II. The density of the silver metal is 10.49 g/mL at 15°C.[24]

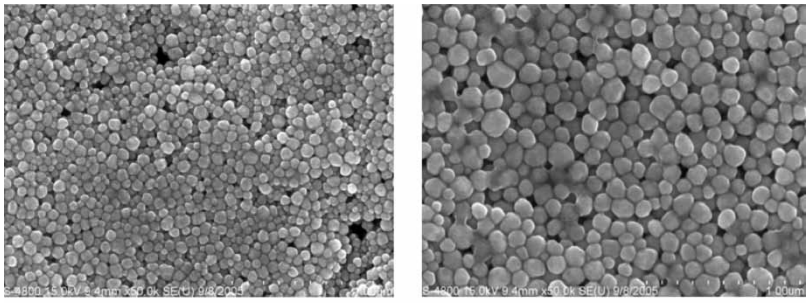

Figure 1. FE-SEM images of batch I and II of silver nanoparticles.

Sedimentation Field-Flow Fractionation (SdFFF)

The SdFFF channel is 0.0127 cm thick, 89.1 cm long and 1.1 cm wide. The radius of the channel rotor is 15.1 cm. The channel void volume was measured from the elution volume of acetone to be 1.33 mL. The carrier solution was pumped by Futecs NS-4000 GP gradient pump (Daejeon, Korea). The flow rate was measured by an Optiflow 1000 Liquid Flowmeter (Agilent Technologies, Palo Alto, USA). The elution of the sample was monitored by a UV-106 UV/VIS detector (Linear Instruments, Reno, USA) with the wavelength fixed at 254 nm. The control of the SdFFF system and the data collection/processing was performed by a personal computer loaded with the software provided by Postnova USA (Salt Lake City, Utah, USA). The carrier liquid was water containing 0.1% (w/v) FL-70 (Fisher Scientific, Fair Lawn, NJ, USA). All samples were directly injected through a septum into the channel. The injection volume was 5∼30 μL, depending on the sample concentration. The sample suspensions were vortexed for 30 sec before the injection. All experiments were performed at room temperature.

Field Emission-Scanning Electron Microscopy (FE-SEM)

A Hitachi S-4800 (Tokyo, Japan) field emission scanning electron microscope (FE-SEM) was used to analyze the silver nanoparticles at the acceleration potential of 15 kV (resolution = 1.0 nm).

RESULTS AND DISSCUSSION

SdFFF of Polystyrene Latex Beads

Figure 2 shows the overlaid fractograms and the size distributions obtained by SdFFF for 222, 300, and 502 nm polystyrene latex beads. The flow rate was the same for all three standards at 1 mL/min. The channel rotation rate was 1600, 1400, and 700 rpm for 222, 300, and 502 nm particles, respectively. The mean sizes determined from the first moment of the size distributions shown in Figure 2 are summarized in Table 1. The SdFFF data are in excellent agreements with the nominal diameters with the relative errors less than 2%.

Selection of SdFFF Carrier Liquid

Appropriate choice of the carrier liquid is required in SdFFF to avoid unwanted charge interactions that could cause adsorption or repulsion

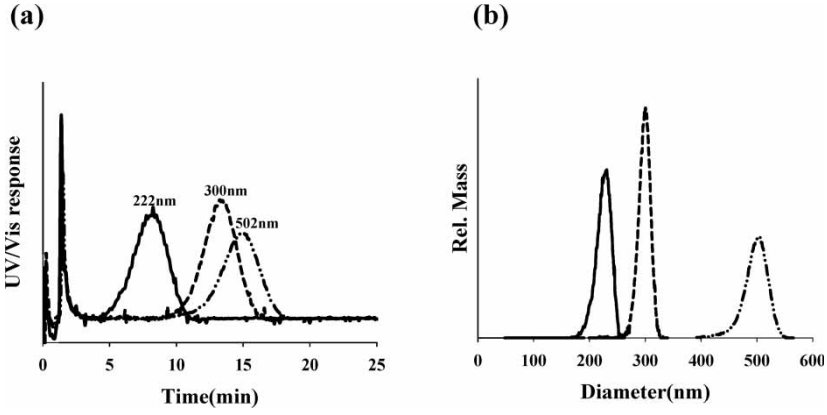

Figure 2. SdFFF fractograms (a) and size distributions (b) of 222, 300, and 502 nm polystyrene latex beads obtained at the field strength of 1600, 1400, and 700 rpm, respectively. The flow rate was 1 mL/min.

between particles or between the particles and the channel surface.[25–27] Figure 3 shows SdFFF fractograms of sample D (20:80 mixtures of batch I and II) obtained with aqueous carriers of various compositions at the same experimental conditions. The channel rotation rate (field strength) was 1100 rpm and the flow rate was 3 mL/min. In pure water, only one peak is shown, probably due to co-elution of the two populations, batch I and II. In water with 0.1% FL-70 + 0.02% NaN_3 or with 0.1% SDS, the fractograms show severe tailings. In water with 0.1 or 0.2% FL-70, the fractograms show two populations partially separated, with slightly better resolution in water with 0.1% FL-70. Water with 0.1% FL-70 was chosen as the carrier liquid for all SdFFF analysis of silver nanoparticles in this study.

SdFFF of Silver Nanoparticles

Figure 4a shows SdFFF fractograms of the samples A∼E obtained at the same experimental conditions as those in Figure 3. As explained with

Table 1. Mean diameters of polystyrene latex beads measured by SdFFF

Nominal diameter (nm)	Measured diameter (nm)	Relative error (%)
222	226	1.8
300	298	0.7
502	500	0.4

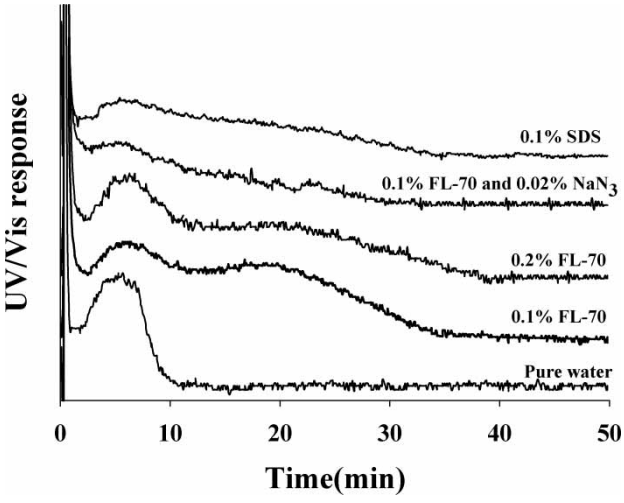

Figure 3. SdFFF fractograms of sample D (20/80 mixture of batch I and II) obtained with aqueous carriers of various compositions. Experimental conditions: field strength, 1100 rpm; flow rate, 3 mL/min.

Eq. (5), the SdFFF fractogram can be directly converted to a size distribution if the density is known. The size distributions converted from the fractograms shown in Figure 4a are shown in Figure 4b. The density of 10.5 g/mL was used in all size calculations in this study. The size distributions of sample A and E shown in Figure 4b yields the mean diameter of 69 and 102 nm, respectively.

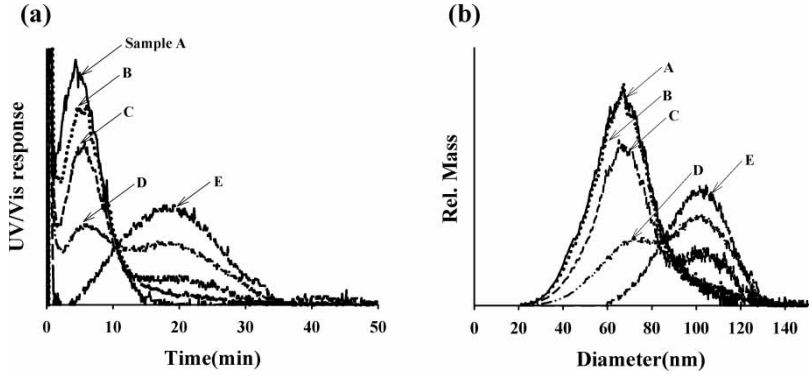

Figure 4. SdFFF fractograms (a) and size distributions (b) of silver nanoparticle sample A∼E. Both fractograms and size distributions are area normalized. Experimental conditions are the same as those in Figure 3.

For mixtures B, C, and D, separation of batch I and II are not complete, probably due to the broadness in size distributions of batch I and II. The Peak-fit^{TM} (SPSS, Chicago, USA) software was used to mathematically deconvolute the fractograms of the samples B, C, and D. First, various functions were tested to fit the fractograms of the samples A and E, and the results are listed in Table 2, where R^2 (coefficient of determination) is one minus the ratio of the sum of squares due to error to the sum of squares about the mean, SE (standard error) is the root mean square error, and F is the ratio of mean square regression to the mean square error. Among various functions tested, the 'lognormal-4 area' was chosen as it yielded the highest R^2 and the lowest SE.

Figures 5a and b shows plots of the mass vs. SdFFF peak area measured for the batch I and batch II of the silver nanoparticles, respectively. All the experimental conditions were the same as those in Figure 3. In both Figures 5a and b, the filled circles are measured data and the lines are the results of the first order least square fitting of the data. For both batch I and II, the relationship between the mass and the peak area shows good linearity with R^2 (correlation coefficient) values of 0.9660 and 0.9832 for batch I and II, respectively.

The lines shown in Figure 5 were used to determine the mass content of batch I and II in mixtures B, C, and D, and the results are shown in Table 3. The mass percentage of batch I/II were determined to be 70/30, 39/61, and 30/70 for the sample B, C, and D, respectively, which show an error of about 10%. This error is attributed to combination of various causes, including the incomplete separation of the mixtures (due to broadness in size distributions of each batch and the band broadening during SdFFF elution) and imperfect fitting of the fractograms.

In FFF, field programming[17,19,28,29] or flow programming,[30–32] where the field strength or the flow rate is changed during separation, may be used to increase the resolution (R_s), to avoid excessive retention of a larger component, and to improve detectability. SdFFF fractograms of the sample F obtained by flow programming are shown in Figure 6, along with that obtained at a constant flow rate. The field strength was maintained at 800 rpm during all experiments. In the flow programming A∼D, the flow rate was maintained at 2 mL/min during the first 2 min, and then was linearly increased until it reaches 4 mL/min at A 10, B 20, C 30, and D 40 min. The resolution (R_s) and the separation time measured for the fractograms shown in Figure 6 are summarized in Table 4. As shown in Table 4, the separation times in the flow programmed runs A∼E (40∼46 min) were shorter than in the constant flow rate run (60 min). The loss in the resolution by the flow programming seems to be insignificant. Based on the results shown in Figure 6 and in Table 4, the flow programming B yielded the best separation among the elution methods tested.

Figure 7 shows SdFFF fractograms of the sample F obtained by (A) a flow programming and by (B) a field and flow dual programming. In both (A) and

Table 2. Peak-fitting parameters of batch I (sample A) and II (sample E) of silver nanoparticles

	Sample A			Sample E		
Fitting function	R^2	*SE*	*F*	R^2	*SE*	*F*
Gauss area	0.956537	11.8649	3928.46	0.939529	7.24304	7434.32
HVL (haarhoff-Van der Linde)	0.957483	11.7516	2672.37	0.925953	8.01914	3984.88
NLC (non-linear chromatogrphy)	0.937807	14.2130	1789.36	0.86559	10.8041	2052.19
Giddings	0.937808	14.1929	2691.65	0.938157	7.32471	7258.85
EMG (exponentially modified gaussian)	0.958454	11.6166	2737.63	0.942468	7.06849	5220.29
GMG (half-Gaussian modified gaussion)	0.958430	11.620	2735.95	0.943968	6.97574	5368.57
EMG + GMG	0.958603	11.6121	2055.10	0.942896	7.04584	3942.23
GEMG 4-parm (4 parameter EMG-GMG hybrid)	0.958491	11.6114	2740.15	0.943406	7.01067	5312.03
GEMG 5-parm (5 parameter EMG-GMG hybrid)	0.958491	11.6278	2049.34	0.943406	7.01434	3979.86
Log normal-4 area	0.958917	11.5517	2769.77	0.944779	6.92510	5425.06
EVal4 area tailed (extreme value 4 parameter tailed)	0.958886	11.5561	2767.61	0.944673	6.93174	5441.00
Eval4 area fronted (extreme value 4 parameter fronted)	0.948993	12.879	2205.10	0.925915	8.02118	3982.69

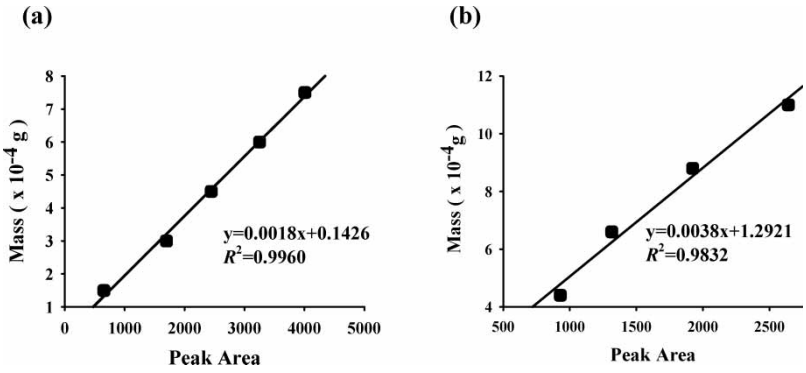

Figure 5. Plots of mass vs. peak area for silver nanoparticles batch I (a) and II (b).

Table 3. Relative mass percentage of batch I and II of silver nanoparticle in mixtures B, C, and D determined by mathematical deconvolution

	Batch I			Batch II		
Sample	Peak area	Mass ($\times 10^{-4}$ g)	%	Peak area	Mass ($\times 10^{-4}$ g)	%
B	2011.7	3.76	70.2	80.3	1.60	29.8
C	436.5	0.93	38.9	43.9	1.46	61.1
D	916.1	1.79	29.7	776.3	4.24	70.3

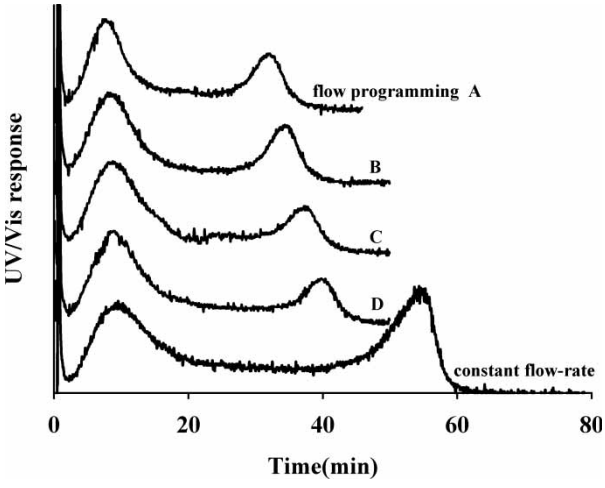

Figure 6. SdFFF fractograms of sample *F* obtained at 800 rpm by flow programming. Flow rate was 2 mL/min at the beginning, and after 2 min, the flow rate was increased linearly until it reaches 4 mL/min in 10, 20, 30, and 40 min for A, B, C, and D, respectively.

Table 4. Resolution and separation time measured for fractograms shown in Figure 6

Elution method	Resolution (R_s)[a]	Separation time (min)
Flow-programmed		
A	1.94	40
B	2.08	42
C	2.02	44
D	2.05	46
Constant flow	2.09	60

[a]R_s was determined by $R_s = (b - a)/(\alpha + \beta)$, where a and b are the elution times of peak 1 and 2, α and β are the half-with of the peak 1 and 2, respectively.

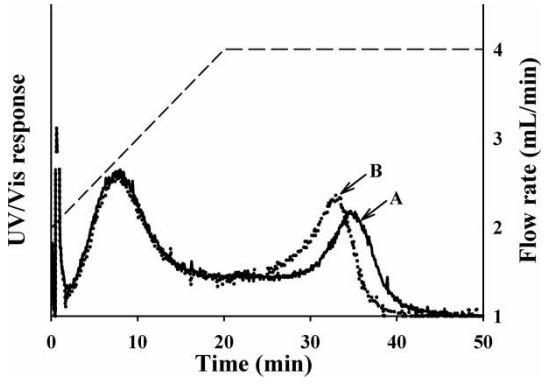

Figure 7. SdFFF fractograms of sample *F* obtained by a flow programming with the field strength fixed at 800 rpm (A) and by a field and flow dual programming (B). The flow rate is represented by the dashed line. In dual programming, the field strength was increased by a power programming with the initial field strength, t_a, t_i, and p of 800 rpm, -160 min, 20 min, and 8, respectively.

(B), the flow rate was linearly increased from 2 to 4 mL/min for the first 20 min, after which the flow rate was kept constant at 4 mL/min. In (A), the field strength was maintained at 800 rpm, while, in (B), the field strength was gradually reduced according to a power function[28] with the initial field strength of 800 rpm, t_a of -160 min, t_i of 20 min, and p of 8. No significant differences in both resolution and in the separation time were found between the flow programming and the field and flow dual programming. The resolution was 1.71 and 1.62 in the flow programming and in the dual programming, respectively.

CONCLUSION

SdFFF was used to separate bimodal mixtures of silver nanoparticles and to determine the size distributions. A flow programming, where the flow rate was linearly increased during separation, provided faster separation than the run at a constant flow rate without losing much in resolution. A field and flow dual programming did not improve much in both resolution and the separation time. Partially separated fractograms were mathematically deconvoluted to determine the relative mass content of the mixtures. With more work for further optimization, SdFFF may provide a useful tool for separation and characterization of various metal nanoparticles.

ACKNOWLEDGMENTS

This study was financially supported by LG chemicals. Dong Young Kang acknowledges the fellowship of the BK21 program from the Ministry of Education and Human Resources Development.

REFERENCES

1. El-Sayed, M.A. Acc. Chem. Res. **2001**, *34*, 257–264.
2. Narayanan, R.; El-Sayed, M.A. Nanoletters **2004**, *4*, 1343–1348.
3. Zhu, J.J.; Liu, S.W.; Palchik, O.; Koltypin, Y.; Gedanken, A. Langmuir **2000**, *16*, 6396–6399.
4. Pillai, Z.S.; Kamat, P.V. J. Phys. Chem. B **2004**, *108*, 945–951.
5. Jiang, H.Q.; Manolache, S.; Wong, A.C.L.; Denes, F.S. J. Appl. Polym. Sci. **2004**, *93*, 1411–1422.
6. Hirano, S.; Wakasa, Y.; Saka, A.; Yoshizawa, S.; Oya-Seimiya, Y.; Hishinuma, Y.; Nishimura, A.; Matsumoto, A.; Kumakura, H. Physica C **2003**, *392*, 458–462.
7. Zhang, J.P.; Chen, P.; Sun, C.H.; Hu, X. J. Appl. Catal. A **2004**, *266*, 49–54.
8. Chimentao, R.J.; Kirm, I.; Medina, F.; Rodriguez, X.; Cesteros, Y.; Salagre, P.; Sueiras, J.E. Chem. Commun. **2004**, 846.
9. Giddings, J.C. Sep. Sci. **1966**, *1*, 123–125.
10. Giddings, J.C. Science **1993**, *260*, 1456–1465.
11. Park, Y.H.; Kim, W.-S.; Lee, D.W. J. Liq. Chromaatogr. & Rel. Technol. **1997**, *20*, 2599–2614.
12. Benincasa, M.A.; Giddings, J.C. Anal. Chem. **1992**, *64*, 790–798.
13. Ratanathanawongs, S.K.; Shiundu, P.M.; Giddings, J.C. Colloids Surf A: Physicochem. Eng. Aspects **1995**, *105*, 243–250.
14. Barman, B.N.; Ashwood, E.R.; Giddings, J.C. Anal. Biochem. **1993**, *212*, 35–42.
15. Zhang, J.; Williams, P.S.; Myers, M.N.; Giddings, J.C. Sep. Sci. Technol. **1994**, *29*, 2493–2522.
16. Anger, S.; Caldwell, K.; Niehus, H.; Muller, R.H. Pharm. Res. **1999**, *16*, 1743–1747.
17. Kim, W.-S.; Park, Y.H.; Shin, J.Y.; Lee, D.W. Anal. Chem. **1999**, *71*, 3265–3272.
18. Cardot, P.; Rasouli, S.; Blanchart, P.J. Chromatogr. A **2001**, *905*, 163–173.

19. Van-Quynh, A.; Blanchart, P.; Battu, S.; Clédat, D.; Cardot, P.J. Chromatogr. A **2006**, *1108*, 90–98.
20. Larry, E.O.; Smith, G.A. Langmuir **1998**, *4*, 144–147.
21. Moon, M.H.; Giddings, J.C. Anal. Chem. **1992**, *64*, 3029–3037.
22. Giddings, J.C.; Yang, F.J.F.; Myers, M.N. Anal. Chem. **1974**, *46*, 1917–1924.
23. Giddings, J.C.; Myers, M.N.; Caldwell, K.D.; Pav, J.W. J. Chromatogr. **1979**, *185*, 261–271.
24. Budavari, S. *The Merck Index*, 12th Edn.; 1996, 1461.
25. Dalas, E.; Koutsoukos, P.; Karaiskakis, G. Colloid & Polym. Sci. **1990**, *268*, 155–162.
26. Park, Y.H.; Kim, W.-S.; Lee, D.W. Anal. Bioanal. Chem. **2003**, *375*, 489–495.
27. Yasushige, M.; Kazuyoshi, K.; Masataka, T. Anal. Chem. **1990**, *62*, 2668–2672.
28. Williams, P.S.; Giddings, J.C. Anal. Chem. **1987**, *59*, 2038–2044.
29. Kim, W.-S.; Park, M.R.; Lee, D.W.; Moon, M.H.; Lim, H.B.; Lee, S. Anal. Bioanal. Chem. **2004**, *378*, 746–752.
30. Giddings, J.C.; Caldwell, K.D.; Moellmer, J.F.; Dickinson, T.H.; Myers, M.N.; Martin, M. Anal. Chem. **1979**, *51*, 30–33.
31. Janouskova, J.; Budinska, M.; Plockova, J.; Chmelik, J.J. Chromatogr. A **2001**, *914*, 183–187.
32. Plockova, J.; Chmelik, J.J. Chromatogr. A **2001**, *918*, 361–370.

Received March 21, 2007
Accepted April 25, 2007
Manuscript 6103